Research Article

Self-built Supercritical CO_2 Anti-solvent Unit Design, Construction and Operation using Carbamazepine

Dan Meng,[1] James Falconer,[2] Karen Krauel-Goellner,[3] John J. J. J. Chen,[1] Mohammed Farid,[1] and Raid G. Alany[2,4]

Abstract. The purpose of this study was to design and build a supercritical CO_2 anti-solvent (SAS) unit and use it to produce microparticles of the *class II* drug carbamazepine. The operation conditions of the constructed unit affected the carbamazepine yield. Optimal conditions were: organic solution flow rate of 0.15 mL/min, CO_2 flow rate of 7.5 mL/min, pressure of 4,200 psi, over 3,000 s and at 33°C. The drug solid-state characteristics, morphology and size distribution were examined before and after processing using X-ray powder diffraction and differential scanning calorimetry, scanning electron microscopy and laser diffraction particle size analysis, respectively. The *in vitro* dissolution of the treated particles was investigated and compared to that of untreated particles. Results revealed a change in the crystalline structure of carbamazepine with different polymorphs co-existing under various operation conditions. Scanning electron micrographs showed a change in the crystalline habit from the prismatic into bundled whiskers, fibers and filaments. The volume weighted diameter was reduced from 209 to 29 μm. Furthermore, the SAS CO_2 process yielded particles with significantly improved *in vitro* dissolution. Further research is needed to optimize the operation conditions of the self-built unit to maximize the production yield and produce a uniform polymorphic form of carbamazepine.

KEYWORDS: anti-solvent; carbamazepine; *in vitro* dissolution; particle size reduction; polymorphism; solid-state; supercritical CO_2.

INTRODUCTION

Over the last decade or so, supercritical fluid technology has been applied to pharmaceuticals for various reasons including the improvement of dissolution behaviour, mainly due to drug particle size reduction, amorphous character and reduced particle size variation. Other methods such as anti-solvent precipitation, spray-drying, melt-extrusion and the mechanical methods such as cutting, attrition and milling have been used to improve dissolution behaviour of drugs by achieving either solid-state transitions and/or particle size reduction (1,2). However, these techniques may have some limitations. For example, typical comminution processes often lead to wide or uneven particle size distributions, heat-sensitive drugs can be degraded and conversion into unwanted or uncontrollable polymorphs can occur (1,2). Furthermore, spray drying processes may cause the precipitated particles to collide and agglomerate within the hot gas media (3). In

addition, inefficient energy consumption and overuse of organic co-solvents, especially for the antisolvent precipitation or surfactants in these operations may pose real or perceived public health and environmental safety issues (4).

Supercritical carbon dioxide (CO_2) treatment of pharmaceuticals has recently received increased attention partly because carbon dioxide is a clean, safe, inexpensive and an environment-friendly solvent. Also, the technique is usually more cost-effective than traditional particle processing methods with respect to energy consumption (5). The particle formation processes involving supercritical CO_2 include the Rapid Expansion of Supercritical Solution (RESS) and supercritical anti-solvent (SAS) methods (6–11). In RESS, the starting material is dissolved in a supercritical fluid and the resultant solution is then rapidly expanded. During this rapid expansion, both the solvent power and density reduce significantly, leading to supersaturation of the solution and subsequent precipitation of solute particles. Gosselin *et al.* examined the possibility of carbamazepine particle micronization using the RESS process, where different polymorphic forms existed in the generated microparticles (12). However, further investigations are constrained by the low solubility of carbamazepine in the supercritical CO_2 phase and a subsequent low microparticle yield (13).

The Supercritical Anti-Solvent (SAS) method is another supercritical CO_2 based process that has been developed to obtain micronized drug particles. In this process, supercritical CO_2 can be used as an anti-solvent if the drug particles of interest show low solubility in the supercritical fluid phase. The

[1] Department of Chemical and Material Engineering, Faculty of Engineering, University of Auckland, Private Bag 92019, Auckland, New Zealand.
[2] Drug Delivery Research Unit (2DRU), School of Pharmacy, University of Auckland, Private Bag 92019, Auckland, New Zealand.
[3] IFNHH, Massey University Wellington, Private Box 756, Wellington, New Zealand.
[4] To whom correspondence should be addressed. (e-mail: r.alany@auckland.ac.nz)

944

drug particles are initially dissolved in a suitable organic solvent and then mixed with the supercritical anti-solvent. Because the supercritical CO_2 has a low dissolving power for the solute but good (or at least partial) miscibility with the organic solvent, the supercritical anti-solvent will diffuse into the organic solvent phase with subsequent evaporation of the organic solvent into the supercritical fluid phase causing the solute to precipitate into fine particles. The net outcome is a decrease in the solute solubility and increase in its concentration in the organic phase. As a result, the organic solution becomes supersaturated and the solute precipitates as fine particles (6,7,14). Particle size distribution can be affected by altering process variables such as pressure and temperature. Other important factors that need to be carefully monitored and attended to are, the miscibility of the solvent and supercritical fluid, organic solvent to supercritical fluid ratio and rate of supercritical fluid addition (15).

A supercritical fluid generally has a diffusivity that can be up to two orders of magnitude higher than that of a liquid phase yet is less than that of a gaseous phase in addition to favorable viscosity and density as shown in Table I (13). This will result in a more efficient mass transfer compared to the conventional liquid–liquid anti-solvent processes and thus supersaturation will happen in a much shorter time scale. Furthermore, the precipitated particles can be easily recovered by washing and drying using the supercritical anti-solvent, with minimal solvent residue in the formed particles.

In this study, the SAS method was applied to carbamazepine (CBZ), a poorly water soluble anti-convulsant drug used in the treatment of certain forms of epilepsy and bipolar disorder (16,17). It displays a dissolution-dependent solubility bio-absorption, and thus labeled a typical *Class* II drug according to the Biopharmaceutical Classification Scheme (BCS) (18). Clinically, carbamazepine exhibits slow and irregular gastrointestinal absorption behaviour after oral administration, due to its slow dissolution rate.

Indeed, Carbamazepine particle's micronization using SAS method has been investigated by several research groups in the past and their data indicated that particle size reduction is possible and different polymorphic or amorphous forms could coexist in the final product (19–21). However, none of the previous studies have managed to relate the particle yield and characteristics with the processing conditions, e.g. temperature and organic solvent/supercritical fluid ratio. It follows that the aims of this paper are to:

- Describe the design and construction of a self-built SAS CO_2 unit and outline the operation conditions required to reduce the particle size of the model class II drug CBZ.
- Investigate the solid state characteristics (crystalline structure, melting behavior, particle size and morphology) of CBZ before and after CO_2 treatment.

Table I. Orders of Magnitude of Diffusivity, Density and Viscosity in Three States of Matter (11)

State	Diffusivity (10^6 m^2/s)	Density (kg/m^3)	Viscosity (10^3kg/m·s)
Gas	10	1	10^{-2}
Supercritical fluid	1	200–1,000	10^{-2}
Liquid	10^{-3}	600–1,600	1

- Compare and contrast the *in vitro* dissolution behaviour of the CO_2 untreated and treated CBZ.

EXPERIMENTAL

Materials

Commercial grade carbamazepine (CBZ) was purchased from Pharm Chemical ShangHai Lansheng Corp (Shanghai, China). Methanol (HPLC grade) was purchased from NZ Alltec Ltd (Auckland, New Zealand) and was used as the alcoholic solvent for CBZ. Liquid CO_2 cylinders (purity 99.99%) were purchased from BOC (Auckland, New Zealand) and were used as the supercritical fluid source.

SAS CO_2 System Design and Construction

The SAS CO_2 anti-solvent system designed, constructed and used in this work is shown schematically in Fig. 1.

The liquid CO_2 was stored in cylinders (No. 1) and was cooled and supplied to the systems using the fluid pump and inner cooler compartment (No.3). The CBZ/methanol solution was delivered by an HPLC pump (model 301, NZ Alltech Inc., Auckland, New Zealand) (No. 4). The cooled CO_2 and the CBZ/methanol solution were mixed in the nozzle assembly unit (No. 7), and the mixture was then fed into the particle precipitation vessel (No. 8). The nozzle assembly and particle precipitation vessel geometry and configuration are outlined in Fig. 2. The nozzel was made of a standard 1/16" stainless steel T-piece with all tubing into and out of the nozzle assembly being of a similar diameter (outer diameter, 1.59 mm and inner diameter, 0.1 mm). The precipitation vessel was made from stainless steel (type 316) for high pressure operation and it has a working space that measures 50 mm in diameter and 65 mm in height. A filter sheet made by sintering pre-alloyed stainless steel powder with a pore size of 0.5 μm was placed inside the precipitation vessel to retain the formed CBZ particles. An O-ring was placed on top of the filter and sealed with salicylic glue to circumvent any leakage inside the vessel and ensure that all particles formed are collected. The precipitation vessel was heated by a heating wire to above the CO_2 critical temperature of 31.1°C. In practice, the heating wire is connected to a temperature controller with an accuracy of ±0.1°C and the vessel is insulated to keep the temperature constant (No. 9 and 10). The system pressure is measured by the pressure transducer (No. 11) and the data is recorded using a desktop computer. A micrometering valve (No. 13) allowed the system pressure to be adjusted. It was kept warm to avoid ice formation which can clog the system. A needle valve (No. 14) is also provided in case of an emergency. In the event that the micrometering valve gets blocked, the needle valve allows the system to be quickly depressurized. All the connecting tubes were made of high pressure-resistant stainless steel (type 316).

SAS CO_2 System Operation Procedure

High pressure liquid CO_2 is preliminarily fed into the system at a constant flow rate (7 or 7.5 mL/min—see Table II)
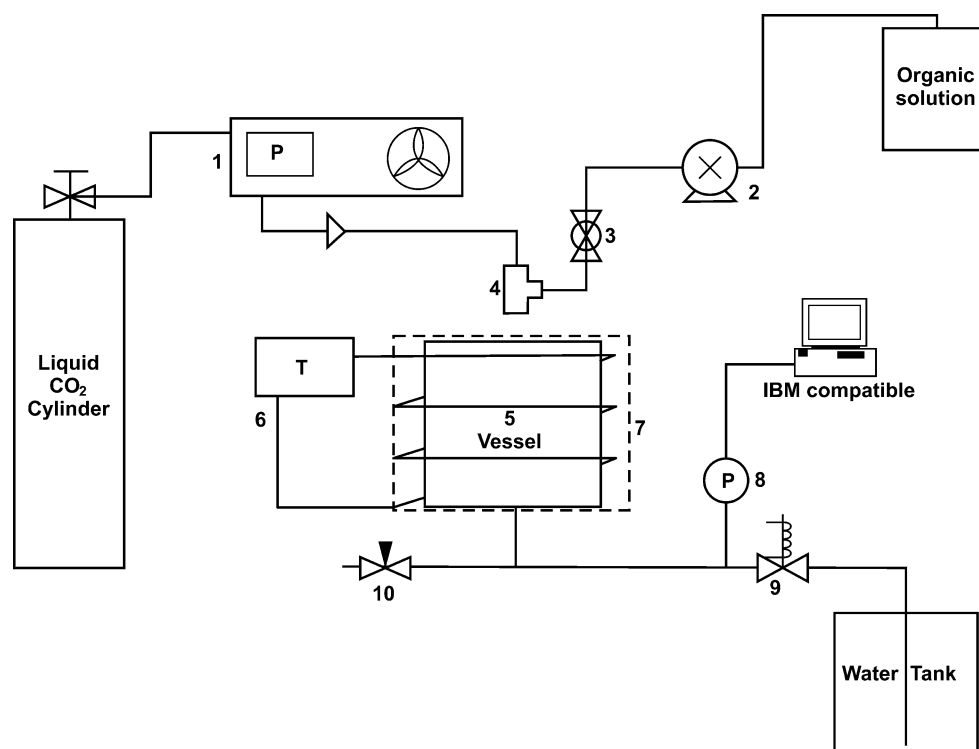
Key: 1. Fluid pump 2. HPLC pump 3. Ball valve   4. Nozzle assembly 5. Particle precipitation vessel
       6. Heating wire 7. Insulation cover (dashed line) 8. Pressure transducer 9. Micrometering valve
       10. Needle valve

Fig. 1. Flow diagram of the supercritical CO_2 anti-solvent system (not to scale)

to remove the atmospheric gases and to increase the system pressure. At the same time, the heating wire starts operation to raise the system temperature to a testing value. After the system conditions reach the CO_2 supercritical state, the desired value of the pressure in the precipitation vessel is attained by regulating the micrometering valve. The experiment starts when the CBZ/methanol (1.5 g/100 mL) solution is fed into the precipitation vessel through the nozzle. After one run, the HPLC pump is turned off and supercritical CO_2 is continually pumped into the vessel to rinse the generated particles for 15 min. This operation was carried out to avoid re-condensation of methanol inside the vessel. The supercritical fluid pump is then stopped and the micrometering valve is fully opened to depressurize the system. When the system pressure decreases to ambient conditions, the vessel is opened and the precipitated particles can be collected from the filter sheet for further analysis.

X-ray Powder Diffraction Studies

X-ray powder diffraction studies (XRPD) analysis for carbamazepine samples were performed with a Bruker D8 Advance powder diffractometer with a Cu Kα radiation ($\lambda=$ 1.5406 Å) (Bruker: Madison, Wisconsin, USA). The scanning angle 2θ ranged from 2° to 40°, and the scan steps were conducted at 0.020° with a counting time of 1 s/step at 33°C. The current and voltage used during operation were 40 mA and 40 kV respectively.
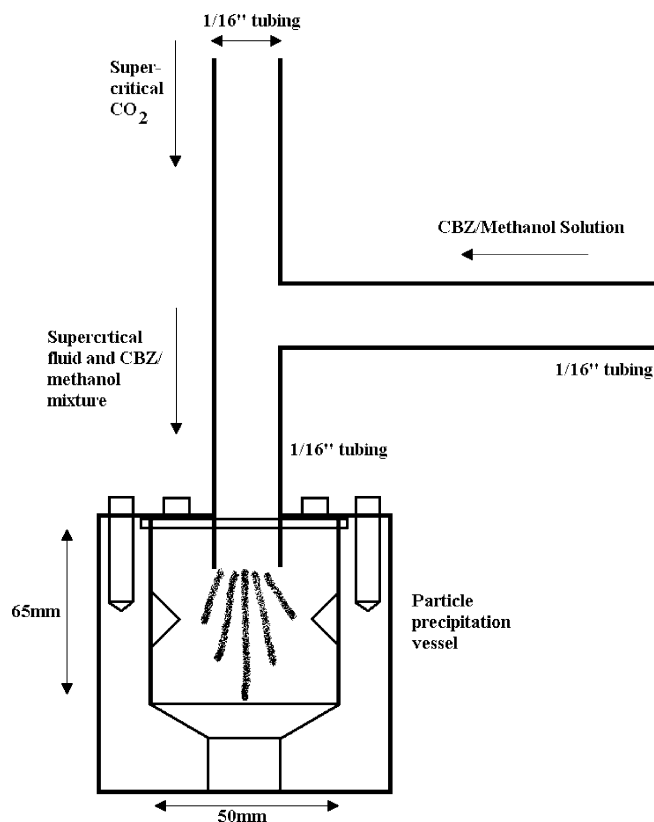

Fig. 2. Nozzle and particle precipitation vessel geometry and configuration

Table II. Production Yield of CBZ Particles Obtained at Different Temperatures and Flow Rate Ratios

System temperature (°C)	CO_2 flow rate (ml/min)	Organic solution flow rate (ml/min)	CO_2/organic solution flow rate ratio	Production yield
33	7.0	0.5	14	0%
33	7.5	0.15	50	73%
36	7.0	0.15	47	50%
37	7.0	0.15	47	42%
40	7.0	0.15	47	19%
40	7.0	0.5	14	0%
40	7.0	0.3	23	Less than 1%
40	10.0	0.3	33	0%
40	11.0	0.3	37	0%
43	7.0	0.15	47	Less than 1%
45	10.0	0.15	67	0%
50	14.0	0.15	93	0%

The yields were calculated using the weight of generated particles divided by the input weight of untreated carbamazepine

Differential Scanning Calorimetry

These studies were performed using a differential scanning calorimetry (DSC) Q1000 differential scanning calorimeter (Intertek ASG Laboratory: Manchester, UK) under nitrogen purge. CBZ samples were accurately weighed in the range of 4.0–7.0 mg and placed into the pin-hole aluminum pans. A non-hermetically sealed aluminum pan with a pin hole in the lid was used as a reference. Thermograms were obtained at a heating rate of 10°C/min over a temperature range of 25–210°C and the sampling frequency was set at 0.2 s.

Scanning Electron Microscopy

The morphology and surface characteristics of CBZ particles were investigated using Scanning Electron Microscopy (SEM) (Philips XL30S FEG: Eindhoven, Netherlands). The samples for SEM were sputter coated with platinum for 180 s at 1.1 kV (Polaron SC 7640 Sputter Coater: Hertfordshire, UK) before viewing under the microscope. The samples had a platinum coating thickness of approximately 75 nm and pictures were taken at 5 kV with a 200 times magnification.

Laser Diffraction Particle Analysis

The particle size and size distribution (PSD) of CBZ samples were examined with the Mastersizer2000 Laser Diffraction Particle Sizer (Malvern Instrument Ltd: UK). For the measurements each sample was dispersed in a 0.1% v/v sodium lauryl sulfate aqueous solution and sonicated during measuring (approximately 60 s).

In Vitro Dissolution Testing

The in vitro dissolution tests were performed according to the rotating paddle method (USP 24) and the dissolution apparatus used was (model SR8PLUS, Hanson Research: CA, USA). The dissolution medium used was 900 mL of fresh Milli-Q water. Samples of SAS CO_2 treated and untreated CBZ (18±0.05 mg) were weighed and dispersed in the pre-equilibrated dissolution medium (temperature=37± 0.2°C) and the paddle was operated at 100 rpm. Dissolution samples of 4 mL were withdrawn every 60 s over the first

10 min, then every 10 min for the following 50 min and replaced with 4 mL of fresh dissolution medium after each withdrawal. Each test sample was filtered using a 0.22 μM filter unit (MillexGS, MF-Millipore MCE Membrane, Corrigtwohill, Ireland) and the absorbance was immediately measured at 285 nm in a UV spectrophotometer (Helios Gamma, Thermo Fisher Scientific, Inc. Waltham, MA, USA). SAS CO_2 treated and untreated samples were tested in triplicates. Statistical analysis of the dissolution results was conducted using a one-way ANOVA with Minitab™ statistical analysis programme Release 12.

RESULTS AND DISCUSSION

SAS CO_2 System Operation Procedure

Carbamazepine (CBZ) was treated by supercritical CO_2 using the anti-solvent technique under various operation conditions. The effects of flow rate ratio and temperature on production yield are outlined in Table II. This investigation focused on the effect of the flow rate ratio (CO_2/organic solution) and temperature on the yield, size and solid state characteristics of the produced CBZ particles.

As shown in Table II a flow rate ratio of 47 led to an acceptable production yield (42–73%) when the operation temperature range was 33–37°C. The yield dropped to 19% when the temperature was raised to 40°C and to negligible amounts (0–1%) for temperatures of up to 50°C. By raising the flow rate ratio at temperatures between 33°C and 37°C, i.e. reducing the proportion of organic solution in the fluid mixture, the supercritical CO_2 anti-solvent environment became more dominant and as a result, the organic solution became supersaturated more readily and as such facilitated particle precipitation. However, higher operation temperatures (43–45°C) compromised the process efficiency as reflected by the negligible production yield values regardless of the flow rate ratio (see Table II).

Nearly all successful particle precipitation occurred at relatively lower temperatures of less than 40°C, which means that a lower temperature favored CBZ particle production. In general, a higher operational temperature can either vaporize the organic solvent easily to achieve a higher degree of supersaturation, or increase the solute solubility and there-

fore impede the precipitation of particles (20,22–24). According to our results, the effect of temperature seemed to prevail in practice. For example, even though the flow rate ratio was increased to 67 or 93, there were no particles found under a high temperature operation (45°C or 50°C) (24). Moreover, other studies have shown that varying the flow rate and varying the nozzle geometry (e.g. the size of the nozzle outlet) had little influence on the particle formation. In fact, a smaller size nozzle (*I.D*=0.1 mm) was found to get blocked more easily and failed in all the particle production trials.

Based on the combined experimental results (those shown in Table II and others that are not shown here), it was concluded that an organic solution flow rate of 0.15 mL/min, carbon dioxide flow rate of 7.5 mL/min, under a pressure of 4,200 psi, over 3,000 s and temperature of 33°C were favorable from a particle yield viewpoint (73%). Therefore only samples processed under these conditions were selected for the particle size and solid state characterization studies. Namely, untreated and SAS CO_2 treated CBZ samples were investigated for changes in the particle size distribution, morphology and crystalline structure. According to the literature, CBZ is known to have at least four anhydrous polymorphic forms: triclinic form (Form I), trigonal form (Form II), monoclinic

form (Form III), and C-centered monoclinic form (Form IV) (21,23,25). O'Brien *et al.* gave a detailed analysis of the four anhydrate polymorphic forms (26).

X-ray Powder Diffraction Studies

Figure 3 (untreated), represents the XRPD pattern of untreated CBZ. It shows a relatively high magnitude of peak intensities and the three highest peaks were in the characteristic positions of 2θ=15.9°, 24.0° and 27.5° respectively, which corresponds well with those reported for the monoclinic form (Form III) (22,23). Conversely, the SAS CO_2 treated CBZ exhibited different peaks that are uncharacteristic of Form III (Fig. 3 treated).

From the XRD results for treated particles it was revealed that the overall magnitude of peak intensities was decreased; indicating that the formed CBZ particles has a decreased crystallinity, increased amorphous character, as well as other polymorphic forms (Fig. 3). In addition, it was noticed that many of the original peaks were either diminished or totally disappeared (2θ=15.9°, 24.0°, 27.5°, 35.0° and 40°). This suggests that the Form III crystals had to some extent transformed after processing. Interestingly several
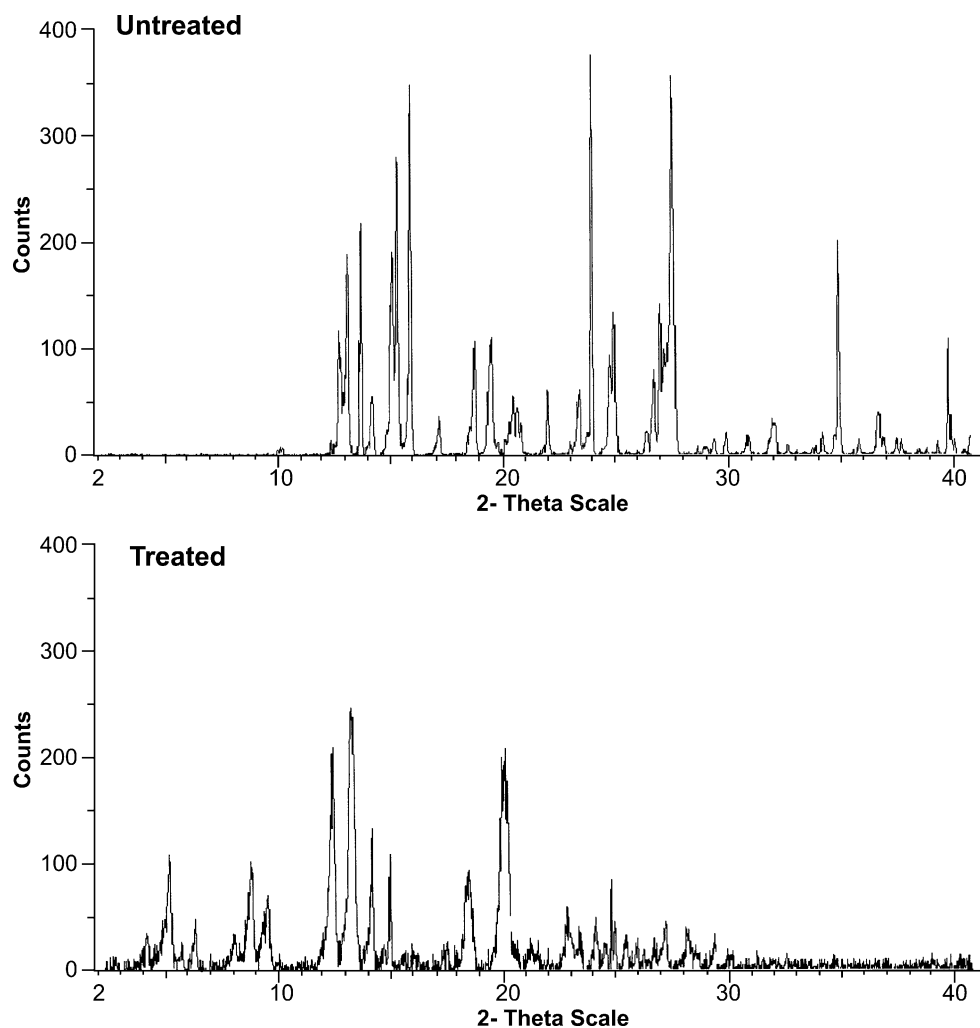

Fig. 3. X-ray powder diffractograms of untreated and treated carbamazepine samples (obtained at 33°C; flow rate ratio of 50)

new peaks did arise at positions that were in good agreement with other reported CBZ polymorphic forms. For example, peaks at $2\theta = 4.9°$, $8.6°$ and $13.3°$ corresponded with those related to the trigonal form (Form II), peaks at $2\theta = 9.3°$ and $12.3°$ with the triclinic form (Form I) and those at $2\theta = 14.1°$ with the C-centered monoclinic form (Form IV) [22,27]. Although the intensities had diminished, the indicative peaks for Form III occur again at $2\theta = 15.9°$ and $24.0°$ in the treated CBZ, with the peak at $27°$ shifting to $27°$ from $27.5°$ (Fig. 3 untreated). These values compare well with the simulated XRD patterns, with the at least one small shift resulting from the different XRD sampling temperatures for data collection [20,27]. However, the intensities vary, especially for form III, which is possibly due to the orientation of powder in the X-ray sample holders as has been reported by other groups [20,27].

Differential Scanning Calorimetry

Figure 4 denotes the thermogram for the untreated and treated CBZ particles. Two characteristic endothermic peaks were identified in the untreated thermogram: A small peak at 170.04°C with an enthalpy of $\Delta H = 8.298$ J/g and a major peak at 192.84°C with an enthalpy of $\Delta H = 136.5$ J/g. These are consistent with those seen in previously published thermal profiles for Form III [27,28]. On the other hand, the thermal profile of the treated CBZ displayed three endothermic peaks: the first at 161.91°C with $\Delta H = 3.725$ J/g, the second at 185.23°C with $\Delta H = 1.432$ J/g and the third melting peak is at 192.41°C with $\Delta H = 142.6$ J/g (Fig. 4—treated).

Changes in the thermal behaviour that are shown in Fig. 4 (treated) corresponded with the different polymorphic forms of CBZ that have emerged after SAS CO_2 treatment
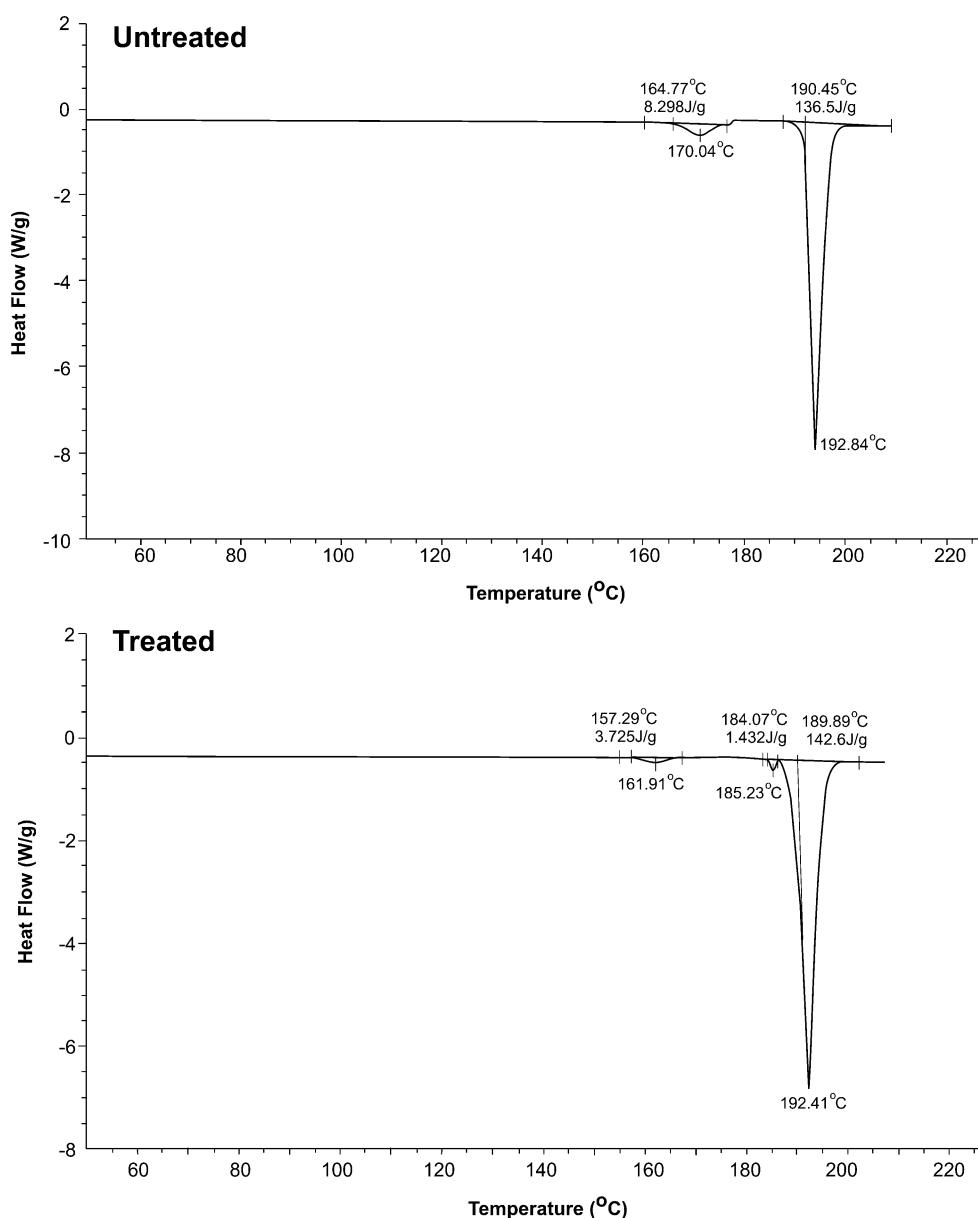

Fig. 4. DSC thermograms of untreated and treated carbamazepine samples (obtained at 33°C; flow rate ratio of 50)

with the unchanged Form III predominating as indicated by the endotherm onset at 164.77°C and the large peak at 192.41°C. The large endotherm observed with an onset of 190.45°C may also be due to the melting of Form I, although it is important to keep in mind that it is possible for Form III to change to Form I when heated and the re-crystallization of Form I from the melt of Form III can be overwhelmed by its melting peak (20). The endothermic peak at 157°C is in agreement with the reported thermal data of Form II whereas the endothermic peak emerging at around 185°C corresponds with Form IV.

Combining both the XRPD and DSC results, it is reasonable to infer that more than one CBZ crystalline forms coexisted in the treated samples with the predominant polymorph being Form III. Such co-existence of different CBZ crystalline forms after SAS CO_2 treatment is very much in agreement with previous reports (20,26,28). The recrystallisation process prevents direct measurement of the enthalpy and quantification of low levels of different forms, especially the higher melting Form I in mixtures of the CBZ crystals is not possible (24). Further investigation is needed to optimize the operation conditions such that only one polymorphic form of CBZ is produced.

The stability of the treated CBZ was not examined, so it is not known whether or not all the new forms of CBZ are converting back to Form III over time. From DSC data it appears that the lowest melting enthalpies of newly formed CBZ are between 1–4 J/g, compared to Form III CBZ of 8.3 J/g. This may indicate that the newly formed CBZ crystals are in a metastable solid state. Further research is needed to monitor the stability of the various crystalline forms of CBZ produced upon SAS CO_2 processing.

Scanning Electron Microscopy

Figure 5 shows the Scanning Electron Micrographs of untreated and treated CBZ at the same magnification. The untreated CBZ particles had a prismatic habit with smooth surfaces. The particles were within the size range of about 200–400 μm (Fig. 5 untreated). On the other hand, micrographs of SAS CO_2 treated CBZ samples showed particle aggregation in the form of bundled whiskers, fibers and filaments (Fig. 5 treated). These emerging morphologies were formed independent of the processing temperature.

From the SEM results the dimension of the treated particles suggested a possible size reduction after processing but was difficult to confirm due to the significant morphological change (prism to fiber) after SAS CO_2 treatment. These findings would again suggest the existence of different (morphologies/polymorphs) which would go in hand with the XRPD and DSC results (Fig. 3). The change in the particle morphology was independent of the operation conditions (flow rate and temperature) and is possibly affected by the nozzle geometry, as this is a well-known factor to influence particle morphology along with the effect of the interfacial phenomena during the process (29).

Laser Diffraction Particle Size Distribution Analysis

Figure 6 (untreated and treated) outlines the particle size distribution for the untreated and the SAS CO_2 treated CBZ samples respectively. For the untreated particles the size distribution parameters were; $d(0.1)$: 41 μm, $d(0.5)$: 182 μm and $d(0.9)$: 419 μm, whereas for the SAS CO_2 treated particles, they measured; $d(0.1)$: 7 μm, $d(0.5)$: 22 μm and $d(0.9)$: 62 μm. It is evident from these results that SAS CO_2 treatment has shifted the overall size distribution to the left i.e. towards a lower particle size (Fig. 6). This is better demonstrated by comparing the surface weighted mean diameter or D[3,2] and volume weighted mean diameter or D[4,3]. The D[3,2] decreased from 87 to 15 μm (17%), whereas the D[4,3] from 209 to 29 μm (14%) after SAS CO_2 treatment.

Another reported advantage for the supercritical fluid technology (in addition to reduced particle size which has implications on dissolution rate) is the increase in mono-dispersity or reduced particle size variation (30). Formation of nanoparticles in supercritical fluids offers significant advantages over conventional liquid-phase systems including rapid separation of solvent and the possibility of depositing the particles *in situ* in porous materials utilizing the unique properties of the supercritical fluid phase (31). The degree of polydispersity can be measured by the "span value" defined as $(d90−d10)/d50$, where dx is the diameter at x% of the cumulative volume size distribution curve (31). The span value obtained for the untreated CBZ was 2.07, while the treated CBZ had a Span value of 2.49. This indicates an
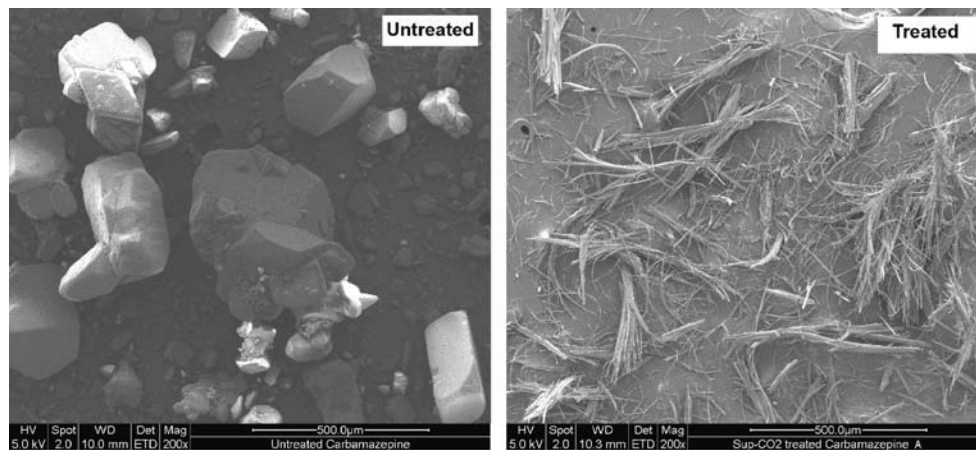

Fig. 5. Scanning electron micrographs of untreated and treated carbamazepine samples (obtained at 33°C; flow rate ratio of 50)
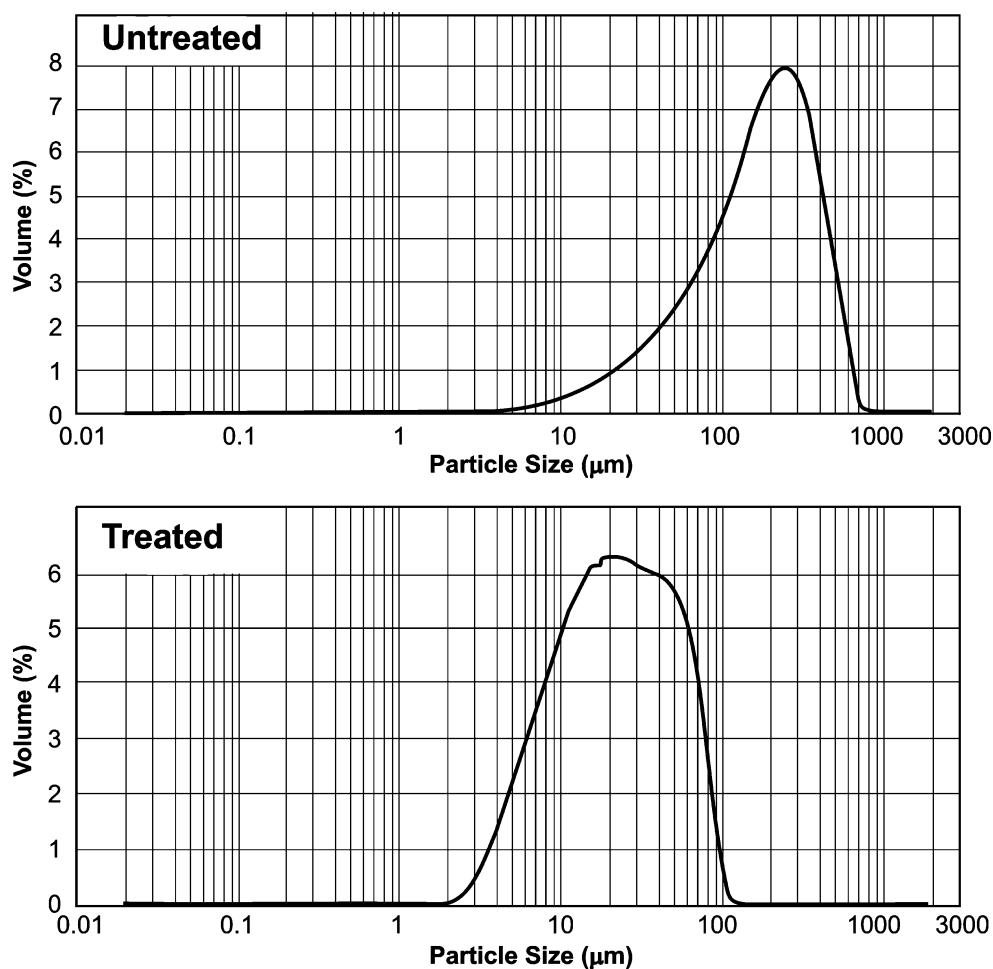
Fig. 6. Particle size distribution results for the untreated and treated carbamazepine

increase in polydispersity. Usually, nanometer-sized particles with a high degree of monodispersity can be obtained using this technology. It is not exactly known why in this experiment the particle size variation has increased, however the different is relatively small and it may be due to incomplete transformation from on one polymorphic form to another. Also, due to incomplete processing the majority of the particles produced are of a smaller size range, however there are still some larger particles remaining in the treated CBZ sample, hence the noticeable variation.
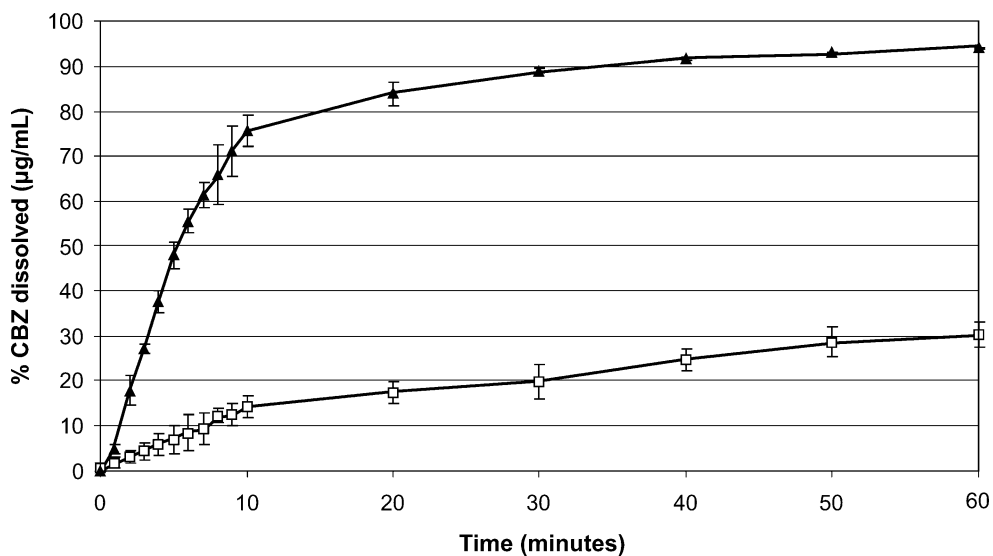

Fig. 7. *In vitro* dissolution profiles of untreated (*open square*) and treated (*closed triangle*) carbamazepine. Results represent means values±SD, $N=3$

In Vitro Dissolution Testing

The *in vitro* dissolution profiles for both untreated and SAS CO_2 treated CBZ samples are shown in Fig. 7. Statistical analysis of the *in vitro* dissolution results using the one-way ANOVA indicated a significant difference between the two profiles (F=17.49, P<0.01). The results, revealed a substantial increase in both the rate and extent of treated CBZ dissolution compared to the untreated samples (Fig. 7). It is evident that 89% of CO_2-processed CBZ was dissolved within 30 min compared to only 20% dissolution of the untreated CBZ at the same time point. This difference in both the rate and extent of dissolution is most probably due to the change in surface area of CBZ particles upon CO_2 treatment. In addition, the improved dissolution can also be attributed to increased amorphous character which in turn increases intrinsic solubility [20,30,32,33].

CONCLUSION

A supercritical anti-solvent (SAS) CO_2 particle processing unit was designed constructed and operated using carbamazepine as a model drug. This unit can be used to reduce the particle size and alter the crystalline structure and subsequently affect the dissolution of carbamazepine. With appropriate modification, this unit can be used for other powdered drug candidates.

REFERENCES

1. A. J. Hickey, and D. Ganderton. Pharmaceutical process engineering, Marcel Dekker, New York, 2001.
2. M. E. Aulton. Pharmaceutics: the science of dosage form design, 2nd ed., Churchhill Livingstone, New York, 2002.
3. K. Okuyama, and I. W. Lenggoro. Preparation of nanoparticles via spray route. *Chem. Eng. Sci.* **58**(3–6):537–547 (2003).
4. E. J. Beckman. Supercritical and near-critical CO_2 in green chemical synthesis and processing. *J. Supercrit. Fluids.* **28**:121–191 (2003).
5. E. L. V. Goetheer, M. A. G. Vorstman, and J. T. F. Keurentjes. Opportunities for process intensification using reverse micelles in liquid and supercritical carbon dioxide. *Chem. Eng. Sci.* **54** (10):1589–1596 (1999).
6. B. W. Wenclawiak, A. Wolf, and S. Wilnewski. Extractability of As-chelates and solubility of different Rh, Pd-chelates in supercritical fluid CO_2. In GHBrunner (ed.), *Supercritical Fluids as Solvents and Reaction Media*, Elsevier, Amsterdam, 2007, pp. 323–340.
7. Y. P. Sun, H. W. Rollins, B. Jayasundera, M. J. Meziani, and C. E. Bunker. In Y. P. Sun (ed.), *Supercritical fluid technology in materials science and engineering: synthesis, properties, and applications*, Marcel Dekker, New York, 2002, p. 491.
8. T. J. Young, S. Mawson, and K. P. Johnston. Rapid expansion from supercritical to aqueous solution to produce submicron suspensions of water-insoluble drugs. *Biotechnol. Prog.* **16**:402–407 (2000).
9. N. Jovanovic, A. Bouchard, G. W. Hofland, G. J. Witkamp, D. J. A. Crommelin, and W. Jiskoot. Stabilization of proteins in dry powder formulations using supercritical fluid technology. *Pharm. Res.* **21**(11):1955–1969 (2004).
10. S. Palakodaty, and P. York. Phase behavioral effects on particle formation processes using supercritical fluids. *Pharm. Res.* **16** (7):976–985 (1999).
11. T. A. Ranjit, and R. B. Gupta. Formation of phenytoin nanoparticles using RESS-SC process. *Int. J. Pharm.* **308**:190–199 (2006).
12. P. M. Gosselin, R. Thibert, M. Preda, and J. N. McMullen. Polymorphic properties of micronized carbamazepine produced by RESS. *Int. J. Pharm.* **252**:225–233 (2003).
13. R. Bettini, L. Bonassi, V. Castoro, Rossi, L. Zema, A. Gazzaniga, and F. Giordano. Solubility and conversion of carbamazepine

14. M. Moneghini, I. Kikic, D. Voinovich, B. Perissutti, P. Alessi, A. Cortesi, F. Princivalle, and D. Solinas. Study of the solid state of carbamazepine after processing with gas anti-solvent technique. *Eur. J. Pharm. Biopharm.* **56**(2):281–289 (2003).
15. J. O. Werling, and P. G. Debenedetti. Numerical modeling of mass transfer in the supercritical antisolvent process. *J. Supercrit. Fluids.* **16**(2):167–181 (1999).
16. S. Budavari, M. J. O'Neil, A. Smith, P. E. Heckelman, and J. F. Kinneary. The Merck index: an encyclopedia of chemicals, drugs and biologicals, 12th ed., Chapman & Hall, London, 1996.
17. K. Parfitt. Martindale: the complete drug reference, 32rd ed., Pharmaceutical, London, 1999.
18. FDA. Waiver of *in vivo* bioavailability and bioequivalence studies for immediate-release solid oral dosage forms based on a biopharmaceutics classification system, 2007. http://www.fda.gov/cder/guidance/3618fnl.pdf (accessed 18/11/07).
19. M. Moneghini, I. Kikic, D. Voinovich, B. Perissutti, and J. Filipovic-Grcic. Processing of carbamazepine-PEG 4000 solid dispersions with supercritical carbon dioxide: preparation, characterisation, and *in vitro* dissolution. *Int. J. Pharm.* **222**(1):129–138 (2001).
20. A. D. Edwards, B. Y. Shekunov, A. Kordikowski, R. T. Forbes, and P. York. Crystallization of pure anhydrous polymorphs of carbamazepine by solution enhanced dispersion with supercritical fluids (SEDS™). *J. Pharm. Sci.* **90**(8):1115–1124 (2001).
21. P. A. Kikic, A. Cortesi, F. Eva, A. Fogar, M. moneghini, B. Perissutti, and D. Voinovich. Supercritical anti-solvent precipitation processes: different ways for improving the performance of drugs. In A. Bertucco (ed.), *Chemical Engineering Transactions, Vol. 2*, AIDIC, Milano, 2002, pp. 821–826.
22. J. C. De La Fuente, C. J. Peters, and A. J. De Swaan. Volume expansion in relation to the gas-antisolvent process. *J. Supercrit. Fluids.* **17**(1):13–23 (2000).
23. J. C. De La Fuente, A. Shariati, and C. J. Peters. On the selection of optimum thermodynamic conditions for the GAS process. *J. Supercrit. Fluids.* **32**(1)–3:55–61 (2004).
24. M. Perrut, J. Jung, and F. Leboeuf. Enhancement of dissolution rate of poorly-soluble active ingredients by supercritical fluid processes Part I: Micronization of neat particles. *Int. J. Pharm.* **288**(1):3–10 (2005).
25. A. Nokhodchi, N. Bolourtchian, and R. Dinarvand. Dissolution and mechanical behaviors of recrystallized carbamazepine from alcohol solution in the presence of additives. *J. Cryst. Growth.* **274**(3–4):573–584 (2005).
26. L. E. O'Brien, P. Timmins, A. C. Williams, and P. York. Use of *in situ* FT-Raman spectroscopy to study the kinetics of the transformation of carbamazepine polymorphs. *J. Pharm. Biomed. Anal.* **36**(2):335–340 (2004).
27. C. McGregor, M. H. Saunders, G. Buckton, and R. D. Saklatvala. The use of high-speed differential scanning calorimetry (Hyper-DSCä) to study the thermal properties of carbamazepine polymorphs. *Thermochim. Acta.* **417**(2):231–237 (2004).
28. A. L. Grzesiak, M. Lang, K. Kim, and A. J. Matzger. Comparison of the four anhydrous polymorphs of carbamazepine and the crystal structure of form I. *J. Pharm. Sci.* **92**(11):2260–2271 (2003).
29. B. Subramaniam, R. A. Rajewski, and K. Snavely. Pharmaceutical processing with supercritical carbon dioxide. *J. Pharm. Sci.* **86**(8):885–890 (1997).
30. R. B. Gupta. Supercritical fluid technology for particle engineering. In U. B. Kompella, and R. B. Gupta (eds.), *Nanoparticle technology for drug delivery, Vol. 159*, Taylor and Francis, New York, 2006, pp. 53–84.
31. H. Ohde, J. M. Rodruguez, X. R. Ye, and C. M. Wai. Synthesizing silver halide nanoparticles in supercritical carbon dioxide utilizing a water-in-CO_2 microemulsion. *Chem. Comm.* **18**:2353–2354 (2000).
32. S. Sethia, and E. Squillante. Solid dispersion of carbamazepine in PVP K30 by conventional solvent evaporation and supercritical methods. *Int. J. Pharm.* **272**:1–10 (2004).
33. B. C. Hancock, and M. Parksi. What is the true solubility advantage for amorphous pharmaceuticals? *Pharm. Res.* **17** (4):397–404 (2000).

polymorphs in supercritical carbon dioxide. *Eur. J. Pharm. Sci.* **13** (3):281–286 (2001).